

Importance of messenger RNA stability of toxin synthetase genes for monitoring toxic cyanobacterial bloom

Xi Li^{a,b}, Donghua Qiu^d, Sheng Chen^{a,b}, Chao Luo^e, Dong Hu^{a,b}, Jie Zeng^{a,b}, Hui Chen^c, Shuai Li^c, Xin Yu^{a,*}

^a Key Laboratory of Urban Environment and Health, Institute of Urban Environment, Chinese Academy of Sciences, Xiamen, 361021, China

^b University of Chinese Academy of Sciences, Beijing, 100049, China

^c Fujian Provincial Investigation, Design & Research Institute of Water Conservancy & Hydropower, Fuzhou, 350001, China

^d Key Laboratory of Marine Biogenetic Resources, The Third Institute of Oceanography SOA, Xiamen, 361005, China

^e College of Petroleum Engineering, Liaoning Shihua University, Fushun, 113001, China

ARTICLE INFO

Keywords:

mRNA stability
Toxin gene
Molecular structure
Quantitative PCR
Colonial cells
Toxic cyanobacterial bloom

ABSTRACT

Toxic cyanobacterial blooms, occurring frequently worldwide, have posed serious threats to human health and aquatic ecosystem. RNA-based quantitative PCR, which could detect potential toxin-producing cyanobacteria that are actively transcribing toxin genes, is a more reliable method, compared to DNA-based qPCR. However, single-stranded mRNA is labile, and their degradation may lead to an underestimate of gene expression level, even misleading toxic risk management, and thus impeding its application. Here, the mRNA stability of microcystin synthetase genes (*mcyA-J*) was systematically evaluated in unicellular and colonial *Microcystis* with various treatments ($-80\text{ }^{\circ}\text{C}$, $-196\text{ }^{\circ}\text{C}$, $4\text{ }^{\circ}\text{C}$ or $25\text{ }^{\circ}\text{C}$ with RNases inhibitors). Results revealed the highly instability of toxin gene transcripts, affected by transcript structures and cell aggregation. The $-196\text{ }^{\circ}\text{C}$ treatment was the most effective for stabilizing these transcripts. RNAstore[®] ($4\text{ }^{\circ}\text{C}$) could stabilize these transcripts effectively for a short time (less than 7 d), but their stability was strikingly reduced in colonial *Microcystis*. Furthermore, decay kinetics of *mcyA-J* transcripts in various treatments was developed, and showed that their decay rates were varied ($0.0018\text{--}3.014\text{ d}^{-1}$), due to different molecular structures. The *mcyH* transcripts had the lowest decay rate (0.0018 d^{-1} at $-196\text{ }^{\circ}\text{C}$), attributed to the fewest AU sites and stem-loops involved in its secondary structure. Thus, *mcyH* was the most proper target gene for monitoring toxic cyanobacterial bloom. These findings provided new insight into mRNA stability of toxin genes, and contributed to monitoring toxic cyanobacterial blooms and water managements using RNA-based molecular techniques.

1. Introduction

Harmful cyanobacterial blooms in eutrophic lakes and reservoirs have been reported all over the world (O'Neil et al., 2012). Many species of cyanobacteria and its cyanotoxins (e.g., microcystin, nodularin, saxitoxins, cylindrospermopsin) have posed serious threats to human health, aquatic animals and aquatic ecosystems (Carmichael, 1992; Paerl and Otten, 2013). Thus, reliable, sensitive and rapid approaches to predict toxin-related risk and monitor toxic cyanobacterial bloom, are strongly essential, and beneficial to establish early warning systems to reduce risk of toxic cyanobacterial blooms (Merel et al., 2013).

Microcystins (MCs) are the most frequently occurred cyanotoxins, produced by a number of cyanobacteria (e.g., *Microcystis* spp., *Nostoc*

spp., *Phormidium* spp., *Anabaena* spp., *Oscillatoria* spp. and *Planktothrix* spp.) (Jungblut and Neilan, 2006; Matthew et al., 2016). The genus *Microcystis* is the most problematic, found in 108 countries, and 79 of which have also reported the MCs (Harke et al., 2016). MCs have been proven to be a potent liver tumor promoter, leading to a serious risk of human health (Falconer et al., 1983; Pearson et al., 2010). Microcystin is synthesized nonribosomally by a large multifunctional enzyme complex. The gene cluster encoding this enzyme complex spanning 55 kb, is composed of 10 bidirectionally transcribed open reading frames arranged in two putative operons (*mcyA-C* and *mcyD-J*). The six *mcyA-E*, *G* genes encode a large multienzyme synthetases, among which *mcyA-C* encode three peptide synthetases, *mcyD* encodes a modular polyketide synthase, and two hybrid enzymes comprising peptide synthetase and the polyketide synthase modules are encoded by *mcyE* and

* Corresponding author.

E-mail address: xyu@iue.ac.cn (X. Yu).

<https://doi.org/10.1016/j.hal.2019.101642>

Received 12 January 2019; Received in revised form 2 July 2019; Accepted 16 July 2019

Available online 25 July 2019

1568-9883/ Published by Elsevier B.V.

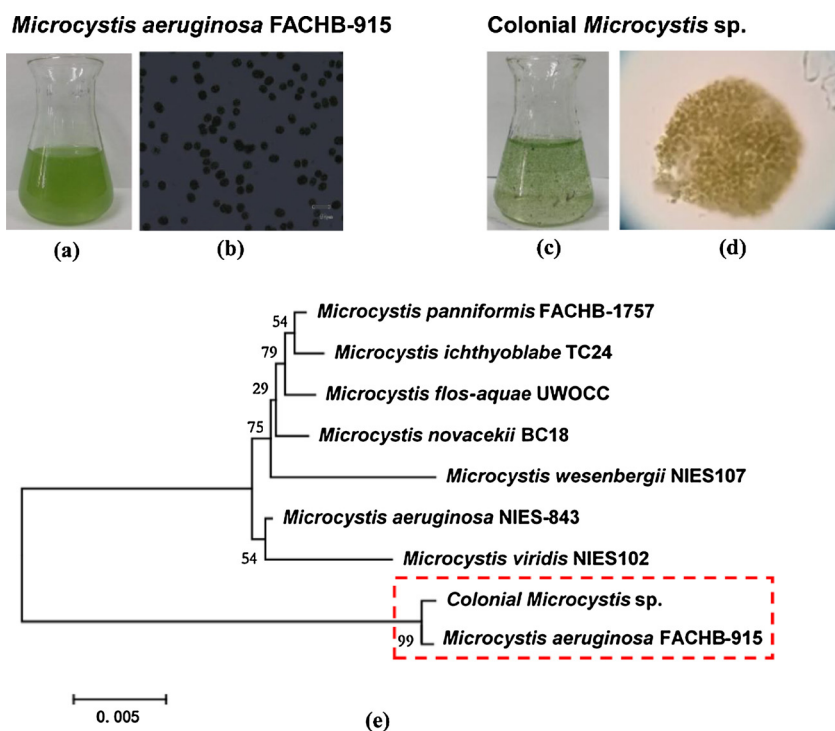


Fig. 1. Comparison of unicellular and colonial *Microcystis*. (a), (c) showing the appearance of cell culture in conical flasks, and (b), (d) showing cell morphology observed by microscope at 400 \times magnification. Phylogenetic tree based on neighbor-joining analysis of 16S rRNA gene sequences of unicellular, colonial *Microcystis* and representatives of some other related taxa by DNAMAN 8.0 software, and bootstrap values showing at branch points (e). Red dashed frame showing the clustering of the unicellular and colonial strains used for experiments in our study (e). (For interpretation of the references to colour in this figure legend, the reader is referred to the web version of this article.)

mcyG. Enzymes putatively involved in the tailoring, are encoded by *mcyF,L,J*, and the transporting of the toxin by *mcyH* (Tillett et al., 2000).

DNA-based quantitative PCR methods (summary in Table S1) have been applied to quantify toxin gene copies to predict potential toxin production in natural freshwaters. Nonetheless, DNA-based methods could only reveal the presence of toxin genes involved in toxin production. For environmental samples, DNA can originate from living and dead cells. Additionally, toxin genes can be mutated, preventing or diminishing their transcription and subsequent toxin production (Kaebernick et al., 2001; Mikalsen et al., 2003; Christiansen et al., 2008). Thus, the DNA-based technique may overestimate toxicogenicity due to little insight of active toxin biosynthesis gene transcription.

RNA-based molecular technique (RT-qPCR, reverse transcription-polymerase chain reaction), which allows the detection of potential toxin-producing cyanobacteria that are alive and actively transcribing the toxin genes, is a more reliable method with high sensitivity for monitoring toxic cyanobacterial bloom. Active *mcyE* gene expression was detectable using RT-qPCR, even though microcystin concentration was very low (below detection limit by ELISA) by Sipari et al. (2010). Expression of biosynthesis genes of nodularin, produced solely by *Nodularia spumigena*, was also detected by qPCR in Baltic Sea samples (Jonasson et al., 2008). However, RNA molecules are more labile than double-stranded DNA molecules. These mRNA could merely remain in cells for a few minutes or hours (Hui et al., 2014). For water resource managers, RNA extraction and RT-qPCR analysis could not be completed on site, and thus, these field samples should be preserved on site, and then, they spend a few hours or days to transport to laboratories for analysis. Inevitably, this process will lead to RNA degradation, resulting in underestimating these toxic genes expression level, and even misleading the toxin risk management in freshwaters.

RNA degradation is mediated by a series of RNases in cells (e.g., PNPase, Rhl B, RNase R, RNase II, RNase J, Degradosome) (Carpousis, 2002, 2007; Luro et al., 2013; Hui et al., 2014). Many factors (e.g., RNA sequence or structural elements, RNases activity, temperature) affect RNA stability. Freezing could affect properties of proteins, nucleic acids by changing hydrophobic and hydrophilic interactions, which determined structure and function (Wolkers et al., 2007), and resulted in a decrease or loss of enzymatic activity (Auer et al., 2014). Commercial

RNases inhibitors (e.g., RNastore[®], RNAlatter[®]) have been widely utilized to inactivate RNases to enhance RNA stability (Camacho-Sanchez et al., 2013; Perez-Portel and Riesgo, 2013). Besides, RNA molecules, which have secondary structures (stem-loop, hairpin) could prevent endonuclease degradation, among which 3' adenylation or 5' stem-loop could protect them against from 3'-5' (e.g., RNase II, PNPase, RNase J) or 5'-3' exonuclease degradation as well (Emory et al., 1992; Xu and Cohen, 1995).

To date, the issue about mRNA stability of toxin genes was ignored by previous studies, although it is critical for monitoring toxic cyanobacterial bloom using RNA-based techniques. In this study, the mRNA stability of microcystin synthetase genes (*mcyA-J*) was systematically evaluated in unicellular and colonial *Microcystis* with various treatments (-80 $^{\circ}$ C, -196 $^{\circ}$ C, 4 $^{\circ}$ C or 25 $^{\circ}$ C after adding RNases inhibitors). Besides, decay kinetics of these transcripts in various treatments were developed, and transcripts structures were analyzed as well. The aims of this study were to (i) explore factors affecting mRNA stability of toxin genes, (ii) find proper toxin target gene for monitoring toxic cyanobacterial bloom, and effective treatments to stabilize the transcripts of these toxin genes.

2. Materials and methods

2.1. Unicellular and colonial *Microcystis* sampling

A toxic strain *Microcystis aeruginosa* FACHB-915 was purchased from the Institute of Hydrobiology, Chinese Academy of Sciences. It was cultured in BG11 medium (Hopebio, China) at 25 $^{\circ}$ C under constant light flux (35 μ mol of photons $m^{-2} s^{-1}$) with a 12 h:12 h light-dark cycle. The strain remained unicellular in laboratory.

Microcystis cells always form colonies in natural freshwaters (Ma et al., 2014), and thus, the effect of cell aggregation on the stability of *mcyA-J* transcripts should be investigated. Colonial samples were collected in Maxi pond located in Shantou (China), where a toxic cyanobacterial bloom occurred in 2018 (Fig. S1). The 16S rRNA gene sequence analysis of the colonial samples revealed that the closest relative was *Microcystis aeruginosa* FACHB-915 with 99.79% similarity and NIES-843 with 99.21% similarity, respectively (Fig. 1). It suggested the

Microcystis sp. was the predominant population in colonial samples.

In this study, the unicellular and colonial *Microcystis* were employed to conduct RNA preservation experiments. However, colonial *Microcystis* was difficult to estimate cell counts using microscopy, attributed to the large irregularly shaped colonies consisted of thousands of cells per colony in a three-dimensional matrix. Thus, chlorophyll a was used to estimate cell density in unicellular and colonial samples. These samples were diluted to a final chlorophyll a concentration ($30 \mu\text{g L}^{-1}$). To collect cells, each sample of a volume of 10 mL was centrifuged at $6000 \times g$ for 5 min, and washed with 0.9 % NaCl twice.

2.2. Various treatments to stabilize transcripts of toxin gene in samples

Cryopreservation ($-80 \text{ }^\circ\text{C}$ freezer and $-196 \text{ }^\circ\text{C}$ liquid nitrogen) had been widely employed for long-term RNA preservation in soil and tissues samples (Rissanen et al., 2010; Andreasson et al., 2013; Auer et al., 2014; Arav et al., 2016). Thus, the cryopreservation treatments were employed to stabilize transcripts of *mcyA-J* and 16S rRNA genes in unicellular and colonial *Microcystis*, respectively.

RNases inhibitors (e.g., RNastore[®]) could inactivate RNases, and had been proven effective to stable RNA molecules in bacteria, yeast and tissues (Dekairelle et al., 2007; Camacho-Sanchez et al., 2013; Perez-Portel and Riesgo, 2013). In this study, RNastore[®] was purchased from TIANGEN Biotech (China). According to manufacturer, intact RNAs were obtained from bacterium *Escherichia coli*, which has been preserved at $4 \text{ }^\circ\text{C}$ after adding RNastore[®] for 1 month or at $25 \text{ }^\circ\text{C}$ for 1 week. For field sampling, this treatment was more convenient than cryopreservation treatments. Thus, the treatments ($4 \text{ }^\circ\text{C}$ and $25 \text{ }^\circ\text{C}$ with RNastore[®]) were employed to stabilize *mcyA-J* transcripts in unicellular and colonial *Microcystis*. After 0, 1, 3, 7, 14 and 28 days of preservation, transcripts copies of *mcyA-J* and 16S rRNA gene were quantified by RT-qPCR analysis.

2.3. RNA extraction from cyanobacterial samples

Before RNAs were extracted from *Microcystis* samples, all experimental supplies were treated by DEPC RNase-free water (Solarbio[®], China). Glass mortar was dried in $60 \text{ }^\circ\text{C}$ temperature-constant oven, which was in preparation for pre-treatment by liquid nitrogen grinding to disrupt cells. Then, RNA was extracted using Spin Column Plant Total RNA Purification Kit (Sangon Biotech, China). Amending procedure was adding RNase inhibitor (ThermoFisher Scientific, USA) to inhibit the activity of RNases, and DNase I (ThermoFisher Scientific, USA) to remove unwanted DNA from cell lysates. RNA purity was evaluated by A_{260}/A_{280} and A_{260}/A_{230} ratio, as summarized in Fig. S2. A_{260}/A_{280} was ranging from 1.8 to 2.1 and A_{260}/A_{230} was about 2.0, demonstrating high-purity RNA samples were gained in this study.

2.4. Primer design

The primers of *mcyA-J* and 16S rRNA gene were designed by 'Primer Premier 5.0' software. The PCR amplification products were analyzed with 1.5% (w/v) agarose gel electrophoresis, and conducted by electrophoresis apparatus (JY600C, China). Then, these products were sequenced by Major biotech (Shanghai, China), and sequence alignment analysis was performed via NCBI database (<https://www.ncbi.nlm.nih.gov/>). Melting curves of these products were further analyzed by ABI 7500 real-time PCR system (Applied Biosystems, USA).

2.5. Establishment of quantitative standard curves

Target toxin genes (*mcyA-J*) were cloned into p7S6 cloning vector, which were used as plasmid standard substances. Eq. (1) was the calculation of gene copy number (N). Individual standard curve was established using 10-fold serial dilutions of single copy plasmid. Amplification efficiency of RT-qPCR was calculated using Eq. (2), and the

range of 90–105 % was credible. The *mcyA-J* transcripts copies were calculated using the regression equation of plasmid standard curves.

$$N = \frac{A \times C}{MW} \quad (1)$$

Where N = plasmid copy number in copies mL^{-1} ; A = constant value 6.02×10^{23} copies mol^{-1} ; C = plasmid concentration in g mL^{-1} ; MW = average molecule weight of plasmid standard substance.

$$E = 10^{-1/S} - 1 \quad (2)$$

Where E = amplification efficiency of RT-qPCR; S = slope of the regression equation of plasmid standard curve.

2.6. RT-qPCR procedures

RNAs were transcribed to cDNAs using TransScript One-Step gDNA Removal, and cDNA Synthesis SuperMix (TransGen Biotech, China). Then, cDNAs were used as templates for RT-qPCR analysis. The qPCRs were performed in triplicates using a SYBR[®] Green I qPCR kit (Takara, Japan). Samples were run in a 96-well reaction plate on the ABI 7500 real-time PCR system. The specific qPCR amplification procedures were as follows: initial denaturation 10 min, $95 \text{ }^\circ\text{C}$, 35 cycles; 30 s, $95 \text{ }^\circ\text{C}$; annealing, 30 s, $50\text{--}58 \text{ }^\circ\text{C}$; elongation 30 s, $72 \text{ }^\circ\text{C}$. (Table S2).

2.7. Transcripts structures analysis

Secondary structures of transcripts were predicted using thermodynamics (Mathews and Turner, 2006), based on the nearest neighbor rules that predict the stability of RNA structure as quantified by folding free energy change (Xia et al., 1998; Mathews et al., 2004). A series of prediction tools (e.g., mfold, RNAfold, RNAstructure) have been developed (Zuker, 2003; Reuter and Mathews, 2010), of which mfold (<http://unafold.rna.albany.edu/>) tool has been widely used in the field of molecular biology, and thus, this tool was employed to predict secondary structures of *mcyA-J* transcripts and 16S rRNA in this study.

For secondary structures of RNA molecules, base pairing could form double-stranded RNA, which is more stable than single-stranded RNA molecules, and thus, single-stranded ratio of *mcyA-J* transcripts was calculated by the Eq. (3). RNase E plays a key role in mRNA degradation, which could cut RNA internally within single-stranded regions that are rich in AU sites with little sequence specificity (Mcdowell et al., 1994). Thus, AU sites in single-stranded RNA molecular were estimated. Furthermore, nucleotides in stem-loops could not be paired and easily degraded, so the stem-loops were calculated as well.

$$\text{Single-stranded ratio (\%)} = \frac{\text{Bases in single-stranded (bp)}}{\text{Total bases of transcripts (bp)}} \quad (3)$$

2.8. Statistical analysis

All experiments were conducted in triplicates. The factors affecting stability of *mcyA-J* transcripts, were analyzed using Pearson correlation coefficient analysis.

3. Results

3.1. Effectiveness of qPCR with primers for detecting microcystin-producing cyanobacteria

To ensure the effectiveness of primers for amplifying *mcyA-J* and 16S rRNA genes, the PCR amplification products were analyzed by agarose gel electrophoresis, and their lengths were ranged from 131 bp to 238 bp (Table S2). Analysis of melting curves of these PCR products demonstrated these primers could amplify *mcyA-J* and 16S rRNA genes without nonspecific products, and the sequences had high similarity (> 99%) with *mcyA-J* and 16S rRNA genes in *Microcystis* spp.

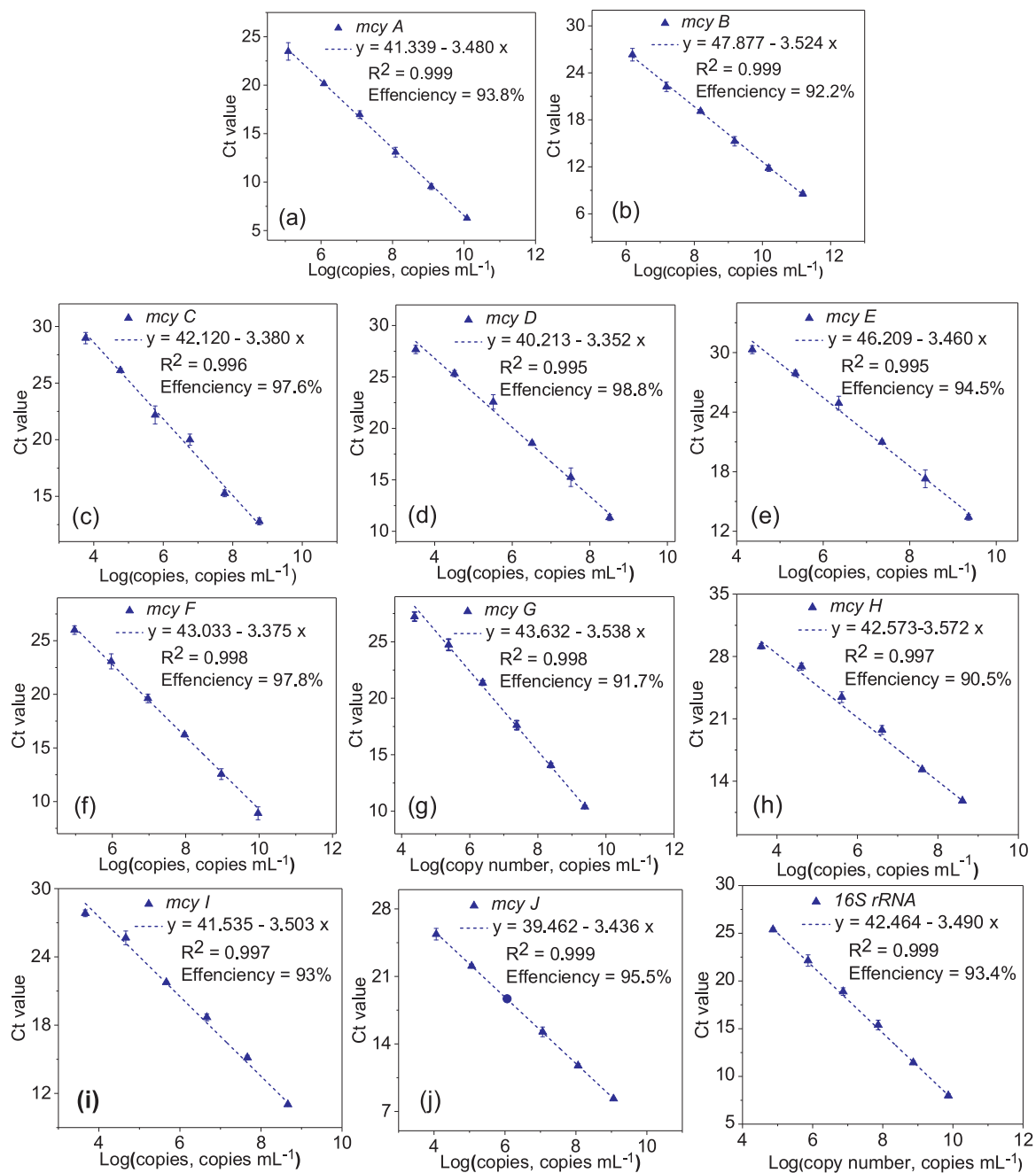


Fig. 2. RT-qPCR standard curves of *mcyA-J* (a-j) and 16S rRNA genes using 10-fold serial dilutions of single copy plasmid. Error bars in the plots representing standard deviation of triplicates. Error bars in the plots represent the standard deviation values.

The quantitative standard curves of transcripts copies of *mcyA-J* and 16S rRNA genes were established. There was a high correlation of CT value and its genes copies ($R^2 = 0.995-0.999$) (Fig. 2). The qPCR amplification efficiency (E) was all greater than 90%, suggesting that the qPCR with these primers for detecting microcystin-producing cyanobacteria in this study, was reliable (Fig. 2).

3.2. Degradation process of *mcyA-J* transcripts in unicellular and colonial *Microcystis* with various treatments

Degradation curves of these transcripts were established in unicellular and colonial samples with various treatments for 28 d (Fig. 3). There was no degradation of the transcripts of 16S rRNA gene in the treatment of -196 °C. In other treatments, these transcripts of 16S rRNA gene and *mcyA-J* were degraded to various extent, and the

degradation process was correlated with preservation time (Fig. 3). Nonetheless, the degradation percentages of *mcyA-J* transcripts were higher than 16S rRNA gene in the same treatment.

For unicellular samples, a rather rapid degradation process of *mcyA-J* transcripts was observed from 0 d to 3 d in treatments of -80 °C and 25 °C preservation with RNAstore[®], and more than 80% of *mcyA-J* transcripts declined at 3 d (Fig. 3). However, the degradation percentages were lower in 25 °C treatment with RNAstore[®] than that at -80 °C. In comparison, degradation process was slowest at -196 °C among the four treatments, and less than 5% of *mcyA-J* transcripts was degraded at 3 d (Fig. 3). When samples were treated at 4 °C with RNAstore[®], the degradation process went through two stages (Fig. 3). A slow process was shown from 0 d to 7 d, among which less than 20% of *mcyA-J* transcripts were degraded (Fig. 3). Then, *mcyA-J* transcripts were degraded rapidly, and degradation percentage reached up to 90% at 28 d.

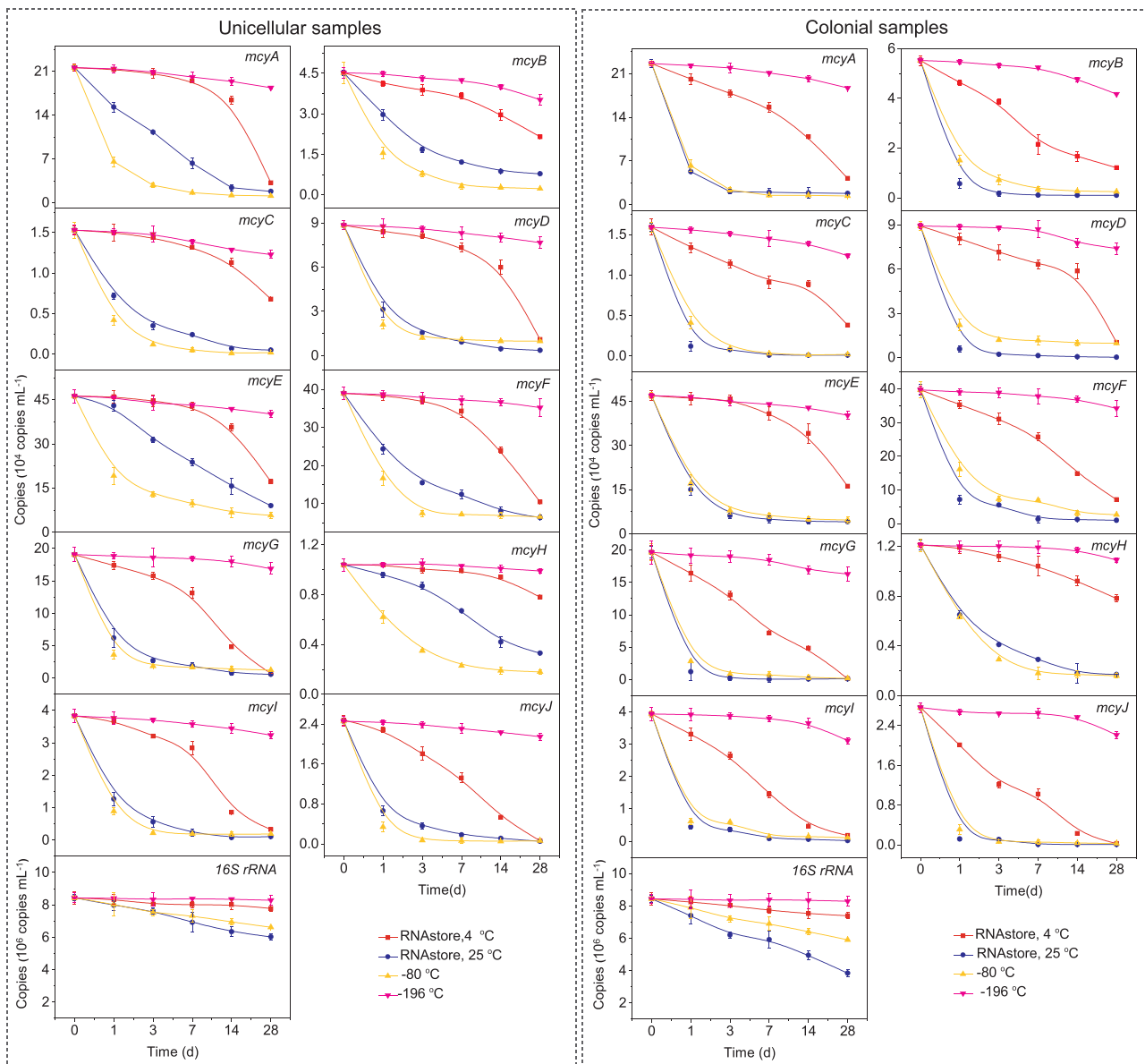


Fig. 3. Degradation process of transcripts of *mcyA-J* and 16S rRNA genes in unicellular and colonial samples with various treatments (-80 °C, -196 °C, 4 °C or 25 °C after adding RNAsore®). Error bars in the plots represent the standard deviation values.

(Fig. 3).

For colonial samples, the degradation process of *mcyA-J* transcripts was slowest at -196 °C, the same as unicellular samples (Fig. 3). Unlike unicellular samples, there was no two stages observed during transcripts degradation in colonial samples at 4 °C treatment with RNAsore®, but a faster degradation process occurred, and more than 60% of *mcyB,E,I,J* were degraded at 7 d (Fig. 3). Furthermore, a rather rapid degradation process was also observed from 0 d to 3d during the treatments of -80 °C and 25 °C after adding RNAsore® (Fig. 3), the same as the degradation pattern in unicellular samples (Fig. 3). However, the degradation percentages were all higher than that in unicellular samples (Fig. 3).

3.3. Kinetics modeling of transcripts degradation in unicellular and colonial *Microcystis*

To estimate the decay rates of transcripts in unicellular and colonial *Microcystis* with various treatments, a first-order kinetics was employed to fit these transcripts copies over preservation time. The fitted

equation was described below (Eq. (4)):

$$\ln\left(\frac{N_t}{N_0}\right) = -kt \tag{4}$$

Where t = preservation time; N_t = transcripts copies after a given preservation time; N_0 = transcripts copies at t = 0 d; and k = decay rate of these transcripts.

Decay kinetics of transcripts of *mcyA-J* and 16S rRNA genes was developed by fitting their transcripts copies (Fig. 4). The models fitted well, and co-efficiencies (R^2) were ranged from 0.805 to 0.999 (Table S3). The degradation rates (k) of *mcyA-J* transcripts were varied from 0.0018 to 3.014 d⁻¹ (Table S3), among which the decay rate of *mcyJ* transcripts was the highest, and *mcyH* was the lowest both in unicellular and colonial samples (Fig. 4). Nonetheless, in the same treatment, the transcripts of 16S rRNA gene had lower decay rate than *mcyA-J* (Fig. 4).

As shown in Fig. 4, decay rates of *mcyA-J* transcripts were lowest at -196 °C among the four treatments, and the corresponding values were 0.0018-0.0092 d⁻¹, 0.0054-0.0100 d⁻¹ in unicellular and colonial

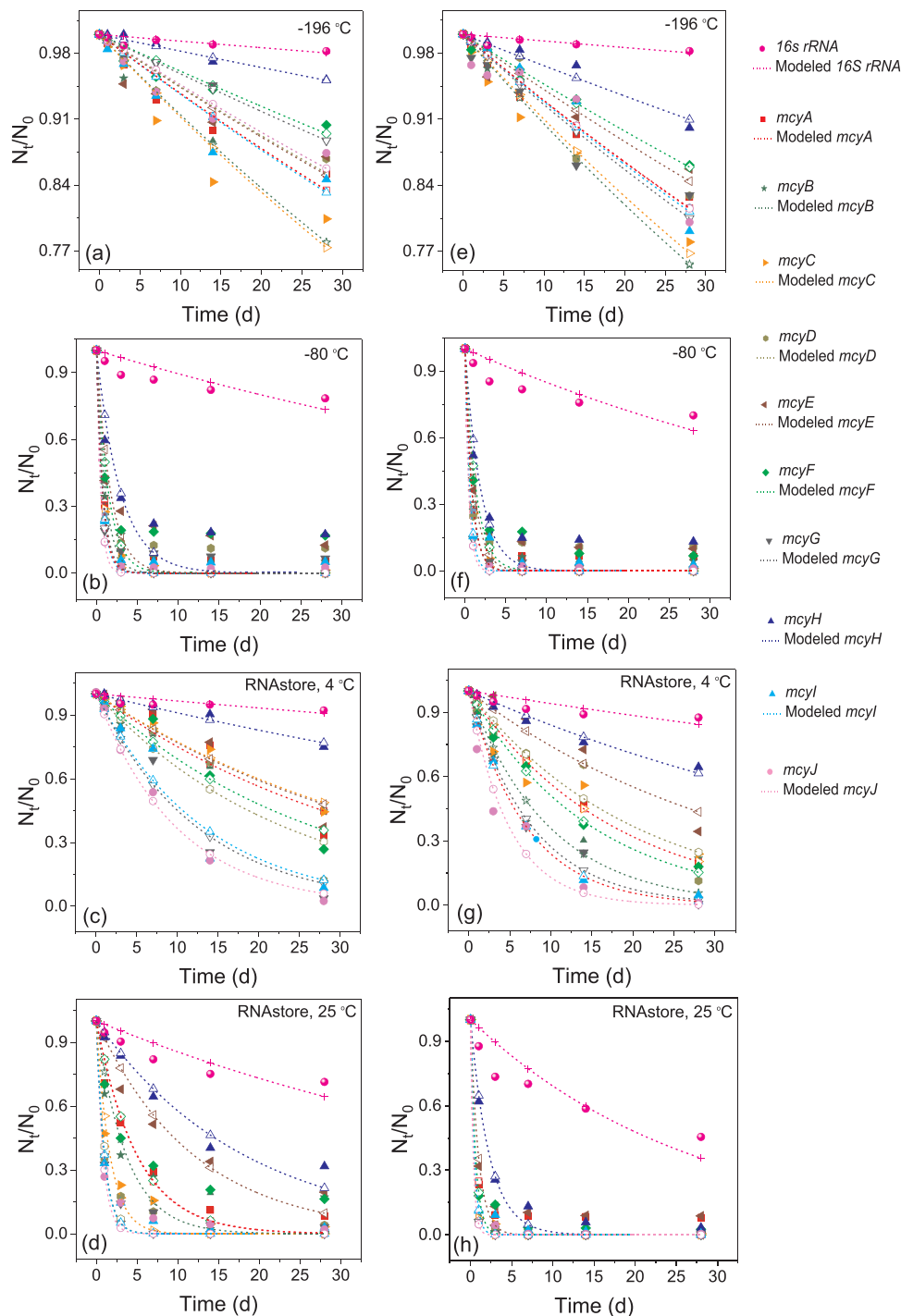


Fig. 4. Kinetics modeling of transcripts degradation (*mcyA-J* and 16S rRNA) in unicellular (a–d) and colonial samples (e–h) with various treatments, including -196°C (a, e), -80 °C (b, f), 4 °C with RNAstore® (c, g), 25 °C with RNAstore® (d, h).

samples, respectively (Table S3). The decay rates of these transcripts were higher at -80 °C than that at 25 °C after adding RNAstore® in unicellular samples, and reversely, the rate was lower in colonial samples (Table S3).

For colonial samples, decay rates of *mcyA-J* transcripts increased to some extent (Fig. 4). Strikingly, the rate of *mcyH* transcripts was 8 times higher than that in unicellular samples with 25 °C treatment after adding RNAstore® (Table S3). Besides, Fig.4f and 4h presented smaller difference of decay kinetics of *mcyA-J* transcripts in colonial samples than that in unicellular samples, due to an increase of decay rates in colonial samples (Fig. 4).

3.4. Transcripts structures analysis of *mcyA-J* and 16S rRNA genes

The primary structures of *mcyA-J* transcripts were differed in sequence and length, of which the sequence length of *mcyH* was the shortest, while *mcyD* was the longest (Table S2, Fig. S3). The secondary structures of *mcyA-J* transcripts were showed in Fig. S3. Particularly, the 3' and 5' of *mcyH* transcripts formed double-stranded molecule (Fig. S3), and it had the fewest of AU sites, stem-loops, and lowest ratio of single-stranded among *mcyA-J* (Table 1). In comparison, *mcyC,J* transcripts had the most AU sites (up to 27) and stem-loops (up to 14), respectively, and *mcyJ* had highest ratio of single-stranded in its

Table 1

Analysis of secondary structural elements of *mcyA-J* transcripts, which were predicted by mfold tool.

Gene	AU site	Stem-loop	Single-stranded ratio (%)
<i>mcyA</i>	18	11	42.4
<i>mcyB</i>	14	12	44.1
<i>mcyC</i>	20	14	39.1
<i>mcyD</i>	23	13	38.7
<i>mcyE</i>	9	9	35.6
<i>mcyF</i>	11	9	60.3
<i>mcyG</i>	19	11	40.1
<i>mcyH</i>	9	7	31.0
<i>mcyI</i>	19	12	36.9
<i>mcyJ</i>	27	10	38.2
16S rRNA	4	9	36.4

transcripts (Table 1). Furthermore, the transcripts of 16S RNA gene had fewer AU sites and stem-loops than *mcyA-J*, but higher ratio of single-stranded than *mcy H* (Table 1).

4. Discussion

4.1. The highly instability of toxin genes (*mcyA-J*) transcripts

Previous studies have demonstrated cryopreservation ($-80\text{ }^{\circ}\text{C}$, $-196\text{ }^{\circ}\text{C}$) was effective for long-term RNA preservation in cells and tissues samples, which kept RNA integrity intact, and endocrine tissue samples could be stored for 27 years at $-80\text{ }^{\circ}\text{C}$ (Andreasson et al., 2013; Auer et al., 2014; Arav et al., 2016). Nonetheless, this study found the *mcyA-J* transcripts were degraded to various extent (5–99 %) in these treatments after 1–7 days of preservation (Fig. 3). In addition, RNAstore® (4 °C, 25 °C), as a short-term RNA preservation for samples, had been proven to be effective for stabilizing RNA molecules in bacteria, yeast and tissues (Perez-Portel and Riesgo, 2013), of which intact RNAs were obtained from bacterium *E. coli*, preserved at 4 °C after adding RNAstore® for 1 month or at 25 °C for 1 week. In our study, *Microcystis* cells are also prokaryotic bacteria. However, a fast degradation of transcripts occurred after 1–3 days of this treatment (Fig. 3), suggesting these transcripts of *mcyA-J* have highly instability.

In addition, the instability of transcripts of *mcyA-J* was higher than 16S rRNA gene with the same treatment (Fig. 4). It could be attributed to the different physiological function of the two genes. The 16S rRNA gene is a house-keeping gene, and its gene expression is less affected by environmental factors than toxin genes (*mcyA-J*). In comparison, toxin genes, as function genes, are active for regulating toxin biosynthesis. Despite there was little knowledge about the mechanism of expression regulation of toxin genes, other studies revealed mRNA stability and degradation regulated by a serious of RNases, is important to orchestrate widespread changes in RNA lifetimes in response to environmental cues (Hui et al., 2014). Thus, the highly instability of *mcyA-J* could be an important mechanism for post-transcription regulation of its gene expression.

4.2. Cell aggregation affecting its stability of toxin genes (*mcyA-J*) transcripts

There was a significant correlation between cell aggregation and the stability of *mcyA-J* transcripts ($r > 0.8$, $p < 0.01$) (Table 2), and decay rates of these transcripts were higher than that in unicellular samples with the same treatment (Fig. 4), suggesting cell aggregation reduced these transcripts stability. Furthermore, for RNAstore® treatment, the increasing ratios of the decay rates of *mcy A-J* transcripts were more striking than that in cryopreservation treatments (Fig. 4). Previous studies reported colonial *Microcystis* cells held stronger capacity of resisting oxidative stress comparing to unicellular cells when treated with chlorine, since colonies cells attached with amorphous mucilage or

Table 2

Effect of cells aggregation on the stability of *mcyA-J* transcripts by Pearson correlation analysis between decay rates of these transcripts in unicellular samples and colonial samples.

	$-196\text{ }^{\circ}\text{C}$	$-80\text{ }^{\circ}\text{C}$	RNAstore, 4 °C	RNAstore, 25 °C
r	0.91	0.97	0.83	0.88
p	0.0018**	0.0003**	0.0004**	0.002**

r: Pearson correlation coefficient.

p: p-value. * $p < 0.05$, ** $p < 0.01$.

sheaths, preventing oxidant permeating (Ma et al., 2014; He and Wert, 2016). Similarly, these colonies may impede the permeation of RNases inhibitors, thus, RNases in cells could not be inactivated sufficiently, especially the inner cells in colonies. Consequently, lower stability of *mcy A-J* transcripts was observed in colonial cells.

4.3. Molecular structures of transcripts affecting its stability of *mcyA-J* transcripts

Pearson correlation coefficient between molecular structures and the stability of *mcyA-J* transcript was analyzed. The sequence length and single-stranded ratio of these transcripts had no correlation with the instability of *mcyA-J* transcripts ($p > 0.05$) (Table S4, S5).

The stem-loops had a significant positive correlation with the instability of *mcyA-J* transcripts in the treatment of $-196\text{ }^{\circ}\text{C}$ ($p < 0.01$) (Fig. 5; Table S6). RNases was in inactivation at this extremely low temperature (Hubel et al., 2014). However, previous studies revealed single-stranded oligoribonucleotides containing UA and CA phosphodiester bonds could be hydrolyzed specifically under non-enzymatic conditions (Bibillo et al., 1999), and the mechanism is found in a wide variety of organisms. In stem-loops, nucleotides could not be paired and remain single-stranded. Thus, the degradation of *mcyA-J* transcripts could be mediated by non-enzymatic hydrolysis in this treatment.

Furthermore, there was a positive significant correlation of AU sites and the instability of *mcyA-J* transcripts ($p < 0.05$), except for the treatment of $-196\text{ }^{\circ}\text{C}$ (Fig. 6; Table S7). Enzymatic reactions are considered to continue at $-80\text{ }^{\circ}\text{C}$ (Auer et al., 2014), and RNases could not be completely inactivated in RNAstore® treatments, due to the special sheath impeding RNAstore® permeating into cells. Besides, previous studies demonstrated that the single-stranded regions that are AU rich, could be recognized, and cut by large amounts of RNase E in cells (McDowall et al., 1994). Thus, the more AU sites involved in *mcyA-J* transcripts, the lower stability of *mcyA-J* was observed.

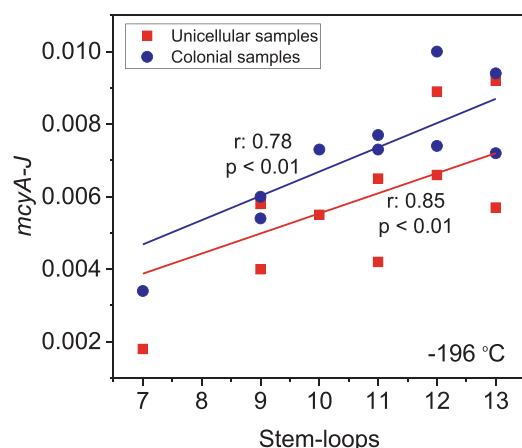


Fig. 5. Effect of stem-loops involved in its secondary structures on mRNA stability of *mcyA-J* in the treatment of $-196\text{ }^{\circ}\text{C}$ by Pearson correlation analysis of stem-loops and the decay rates of *mcyA-J* transcripts. r: Pearson correlation coefficient. p: p-value.

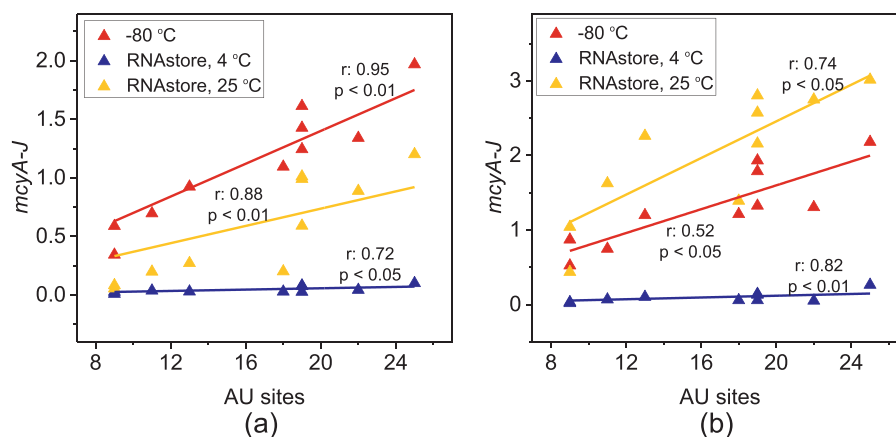


Fig. 6. Effect of AU sites involved in its secondary structures on mRNA stability of *mcyA-J* by Pearson correlation coefficient analysis of stem-loops and the decay rates of *mcyA-J* transcripts. *r*: Pearson correlation coefficient. *p*: *p*-value.

In addition, other molecular structures could be also important for stabilizing these transcripts. For example, transcripts of *mcyH* has the highest stability among *mcyA-J*, because the 3' and 5' terminal of its transcripts forming double-stranded could enhance its stability. Previous studies found 3D structures of RNA molecules, and plenty of non-protein coding short RNAs could also regulate mRNA stability (Czech and Hannon, 2011; Popenda et al., 2012; Aalto and Pasquinelli, 2012; Morris and Mattick, 2014). Thus, the mechanism for regulating the mRNA stability of toxin genes, should be further investigated.

4.4. Effective sample preservation treatments for cyanobacterial samples

The results of this study revealed the highly instability of *mcyA-J*, so the *Microcystis* samples were not proper for long-term RNA preservation. For short-term preservation, $-196\text{ }^{\circ}\text{C}$ treatment was most effective to stabilize *mcyA-J* transcripts. Furthermore, RNAstore[®] treatment was temperature dependent, and $4\text{ }^{\circ}\text{C}$ treatment could slow down RNA degradation process, attributed to the combined inhibition of RNase inhibitors and low temperature. Thus, the treatment of RNAstore[®] (low temperature) could be also employed for short-term RNA preservation in *Microcystis* (1–7 d).

In practice, to monitoring toxic cyanobacterial bloom, a rapid analysis on site is the best, but to date, it is technically limited. Thus, effective treatments for field samples, should be employed to stable *mcyA-J* transcripts. For field sampling, $-196\text{ }^{\circ}\text{C}$ treatment was more effective than RNAstore[®] ($4\text{ }^{\circ}\text{C}$), but was not convenient. Thus, the on-site treatment of RNAstore[®] ($4\text{ }^{\circ}\text{C}$) was suggested, but time-limited (1–3 d), then, these field samples should be analyzed as soon as possible or transferred into $-196\text{ }^{\circ}\text{C}$ in laboratory to prolong preservation time.

In this study, we only investigated the *Microcystis*, which is most problematic, but other genus (e.g., *Nostoc* spp., *Phormidium* spp., *Anabaena* spp., etc.) have been also reported to dominate toxic cyanobacterial bloom. These genera have the same cellular structures (sheath or mucilage surrounding cells). Thus, the effective treatments to stabilize transcripts in *Microcystis*, are also applicable for other genera of cyanobacteria. Furthermore, unlike *Microcystis*, other genera remained unicellular in natural waters, and thus, the same treatment of RNAstore[®] would be more effective for these unicellular cyanobacteria than colonial *Microcystis*. However, other genera or strains are different in cell size, thickness and constituent of cell wall, among which the unicellular cells of the other common toxic genus *Planktothrix* and *Cylindrospermopsis*, are larger than *Microcystis*. Whether these characteristics of species/strains-specific would affect RNA stability of toxin genes, should be further studied.

4.5. Proper toxin target gene for monitoring toxic cyanobacterial bloom

Decay rates of *mcyA-J* transcripts were estimated in various treatments, respectively. (Fig. 4). Results showed their rates were different in the same treatment, among which *mcyH* had the lowest rate (Fig. 4), suggesting its stability of transcripts was highest. In contrast, the stability of *mcyE* was only subordinate to *mcyH* in the treatments of RNAstore[®] and $-80\text{ }^{\circ}\text{C}$, while in the treatment of $-196\text{ }^{\circ}\text{C}$, *mcyF* ranked second (Fig. 4). Besides, *mcyC* and *mcyD* had the lowest stability in the treatment of $-196\text{ }^{\circ}\text{C}$, while the stability of *mcyJ* was the lowest in the treatments of RNAstore[®] and $-80\text{ }^{\circ}\text{C}$ (Fig. 4). It indicated the stability of *mcyA-J* except for *mcyH*, was flexible highly depending on samples treatments. Besides, this study revealed transcripts stability has negative significant correlation of AU sites and stem-loops, and thus, the highest stability of *mcyH* in all treatments, was attributed to the fewest AU sites and stem-loops among *mcyA-J*. Thus, *mcyH* was the most proper target gene for monitoring toxic cyanobacterial bloom using RT-qPCR in all treatments, and the other *mcyA-J*, as proper target genes, should be further evaluated according to specific treatment conditions.

Furthermore, if field samples were analyzed quickly on site, the degradation of these transcripts would be avoided, so, *mcyA-J* are proper toxin target genes for monitoring toxic cyanobacteria bloom. Actually, *mcyA-J* have their own important roles in microcystin biosynthesis. For example, *mcyA-C* encode three peptide synthetases, and the transporting of the toxin is encoded by *mcyH* (Tillett et al., 2000). To our knowledge, whether all of these *mcyA-J* transcripts copies have high correlation with microcystin-producing cyanobacteria, is unknown. Thus, proper *mcyA-J* biomarker for monitoring toxic cyanobacterial should be further assessed by the correlation analysis of *mcyA-J* genes expression and microcystin concentration or microcystin-producing cyanobacteria in natural waters.

Although microcystins (MCs) are the most frequently occurred cyanotoxins, produced by a number of cyanobacteria (e.g., *Microcystis* spp., *Nostoc* spp., etc), other cyanotoxins (nodularin, saxitoxins, cylindrospermopsin) have been reported in natural waters, and are also encoded by corresponding toxin genes (Mihali et al., 2008; Carmichael et al., 1992). This study revealed the transcripts stability of toxin genes (*mcyA-J*) is determined by AU sites and stem-loops involved in their secondary structures. Therefore, to enhance transcripts stability of other target toxin genes, their transcripts should contain AU sites and stem-loops as fewest as possible, which could be predicted by RNA structure prediction tools (e.g., mfold), just as we did successfully in this study.

4.6. Implications for monitoring toxic cyanobacterial bloom

The transcripts of toxin genes have highly instability, but this issue

was ignored by previous studies, and even some conflicting studies was presented by previous literatures. For example, Sipari et al. (2010) implied RNA-based method had high sensitivity for detecting toxin-producing cyanobacteria, since active *mcyE* gene expression was detectable using RT-qPCR when microcystin concentration was very low (preservation condition of field samples: -196°C). However, Ngwa et al. (2014) found *mcyE* transcripts had no correlations with microcystin concentrations (preservation condition: -20°C). The conflicting results may be attributed to highly instability of *mcyE* transcripts at -20°C , as evidenced more than 50% of these transcripts were degraded at -80°C after 1 d in this study. These transcripts degradation could seriously affect the sensitivity of RT-qPCR, and lead to underestimating the toxin genes expression, even misleading toxin risk management. Therefore, transcripts stability was vitally important for monitoring toxic cyanobacterial bloom using RNA-based qPCR.

Molecular biological process occurs earlier than the change of water quality indicators (e.g., cell density, toxin level), since toxin biosynthesis follows a series of steps starting with toxin genes transcription into mRNA. Thus, the monitoring mRNA of toxin genes can actually play a key role in early warning, which is of great significance to take intervention measures in advance and avoid the outbreak of toxic cyanobacterial bloom. However, selecting proper target genes and effective sample preservation treatments are essential prerequisites for establishing a reliable early warning method. Our study has offered suggestions to address this issue, and will provide important references for colleagues in various countries.

5. Conclusions

This study revealed the highly instability of toxin gene transcripts, affected by cell aggregation and molecular structures, but this issue was ignored by previous studies. Among toxin genes, *mcyH* with the highest stability of its transcripts due to the fewest AU sites and stem-loops, was the most proper target gene for monitoring toxic cyanobacterial bloom. The -196°C was the most effective treatment to stabilize these transcripts of toxin genes, and RNAstore[®] (4°C) could effectively stable these transcripts of toxin genes for a short time (1–7 d). Nonetheless, cell aggregation reduced these transcripts stability especially RNAstore[®] treatment. Thus, water resource managers and ecologists should pay more attention to these colonial *Microcystis*. Field analysis of colonial samples maybe necessary, or effective treatments should be employed to stabilize these transcripts of toxin genes.

Declaration of Competing Interest

The authors declare that they have no conflict of interest.

Acknowledgements

This work was supported by National Key R&D Program of China (2017YFE0107300), Science and Technology Project of Water Resources Department of Fujian Province (MSK201711), Science and Technology Major Project of Xiamen (3502Z20171003) and K.C. Wong Education Foundation.[CG]

Appendix A. Supplementary data

Supplementary material related to this article can be found, in the online version, at doi:<https://doi.org/10.1016/j.hal.2019.101642>.

References

Aalto, A.P., Pasquinelli, A.E., 2012. Small non-coding RNAs mount a silent revolution in gene expression. *Curr. Opin. Cell Biol.* 24 (3), 3–40. <https://doi.org/10.1016/j.ceb.2012.03.006>. 333.

Andreasson, A., Kiss, N.B., Juhlin, C.C., Höög, A., 2013. Long-term storage of endocrine

tissues at -80°C does not adversely affect RNA quality or overall histomorphology. *Biopreserv. Biobank.* 11 (6), 366–370. <https://doi.org/10.1089/bio.2013.0038>.

Auer, H., Mobley, J.A., Ayers, L.W., Bowen, J., Chuaqui, R.F., Johnson, L.A., et al., 2014. The effects of frozen tissue storage conditions on the integrity of RNA and protein. *Biotech. Histochem.* 89 (7), 518–528. <https://doi.org/10.3109/10520295.2014.904927>.

Arav, A., Natan, Y., Levi-Setti, P.E., Menduni, F., Patrizio, P., 2016. New methods for cooling and storing oocytes and embryos in a clean environment of -196°C . *Reprod. Biomed. Online* 33 (1), 71–78. <https://doi.org/10.1016/j.rbmo.2016.03.010>.

Bibillo, A., Figlerowicz, M., Kierzek, R., 1999. The non-enzymatic hydrolysis of oligoribonucleotides VI. The role of biogenic polyamines. *Nucleic Acids Res.* 27 (19), 3931–3937. <https://doi.org/10.1093/nar/27.19.3931>.

Camacho-Sanchez, M., Burraco, P., Gomez-Mestre, I., Leonard, J.A., 2013. Preservation of RNA and DNA from mammal samples under field conditions. *Mol. Ecol. Resour.* 13, 663–673. <https://doi.org/10.1111/1755-0998.12108>.

Carmichael, W.W., 1992. Cyanobacteria secondary metabolites—the cyanotoxins. *J. Appl. Bacteriol.* 72, 445–459. <https://doi.org/10.1111/j.1365-2672.1992.tb01858.x>.

Carpousis, A.J., 2002. The *Escherichia coli* RNA degradosome: structure, function and relationship in other ribonucleolytic multienzyme complexes. *Biochem. Soc. Trans.* 30 (2), 150–155. <https://doi.org/10.1042/bst0300150>.

Carpousis, A.J., 2007. The RNA degradosome of *Escherichia coli*: an mRNA-degrading machine assembled on RNase E. *Annu. Rev. Microbiol.* 61 (1), 7187. <https://doi.org/10.1146/annurev.micro.61.080706.093440>.

Christiansen, G., Molitor, C., Philmus, B., Kurmayer, R., 2008. Nontoxic strains of cyanobacteria are the result of major gene deletion events induced by a transposable element. *Mol. Biol. Evol.* 25 (8), 1695–1704. <https://doi.org/10.1093/molbev/msn120>.

Czech, B., Hannon, G.J., 2011. Small RNA sorting: matchmaking for argonauts. *Nat. Rev. Genet.* 12 (1), 19–31. <https://doi.org/10.1038/nrg2916>.

Dekairelle, A.F., Van der Vorst, S., Tombal, B., Gala, J.L., 2007. Preservation of RNA for functional analysis of separated alleles in yeast: comparison of snap-frozen and RNALater[®] solid tissue storage methods. *Clin. Chem. Lab. Med.* 45 (10), 1283–1287. <https://doi.org/10.1515/CCLM.2007.281>.

Emory, S.A., Bouvet, P., Belasco, J.G., 1992. A 5'-terminal stem-loop structure can stabilize mRNA in *Escherichia coli*. *Genes Dev.* 6 (1), 135–148. <https://doi.org/10.1101/gad.6.1.135>.

Falconer, I.R., Beresford, A.M., Runnegar, M.T., 1983. Evidence of liver damage by toxin from a bloom of the blue-green alga, *Microcystis aeruginosa*. *Med. J. Aust.* 1 (11), 511–514.

Harke, M.J., Steffen, M.M., Gobler, C.J., Otten, T.G., Wilhelm, S.W., Woodf, S.A., Paerl, H.W., 2016. A review of the global ecology, genomics, and biogeography of the toxic cyanobacterium, *Microcystis* spp. *Harmful Algae* 54, 4–20. <https://doi.org/10.1016/j.hal.2015.12.007>.

He, X., Wert, E.C., 2016. Colonial cell disaggregation and intracellular microcystin release following chlorination of naturally occurring *Microcystis*. *Water Res.* 101, 10–16. <https://doi.org/10.1016/j.watres.2016.05.057>.

Hubel, A., Spindler, R., Skubitz, A.P.N., 2014. Storage of human biospecimens: selection of the optimal storage temperature. *Biopreserv. Biobank.* 12 (3), 165–175. <https://doi.org/10.1089/bio.2013.0084>.

Hui, M.P., Foley, P.L., Belasco, J.G., 2014. Messenger RNA degradation in bacterial cells. *Annu. Rev. Genet.* 48 (1), 537–559. <https://doi.org/10.1146/annurev-genet-120213-092340>.

Reuter, J.S., Mathews, D.H., 2010. RNA structure: software for RNA secondary structure prediction and analysis. *BMC Bioinformatics* 11 (1), 129. <https://doi.org/10.1186/1471-2105-11-129>.

Jonasson, S., Vintila, S., Sivonen, K., El-Shehawry, R., 2008. Expression of the nodularin synthetase genes in the Baltic Sea bloom-former cyanobacterium *Nodularia spumigena* strain AV1. *FEMS Microbiol. Ecol.* 65 (1), 31–39. <https://doi.org/10.1111/j.1574-6941.2008.00499.x>.

Jungblut, A.D., Neilan, B.A., 2006. Molecular identification and evolution of the cyclic peptide hepatotoxins, microcystin and nodularin, synthetase genes in three orders of cyanobacteria. *Arch. Microbiol.* 185, 107–114. <https://doi.org/10.1007/s00203-005-0073-5>.

Kaebnick, M., Rohrlack, T., Christoffersen, K., Neilan, B.A., 2001. A spontaneous mutant of microcystin biosynthesis: genetic characterization and effect on *Daphnia*. *Environ. Microbiol.* 3 (11), 669–679. <https://doi.org/10.1046/j.1462-2920.2001.00241.x>.

Luro, S., Germain, A., Sharwood, R.E., Stern, D.B., 2013. RNase J participates in a pentapeptide repeat protein-mediated 5' end maturation of chloroplast mRNAs. *Nucleic Acids Res.* 41 (19), 9141–9151. <https://doi.org/10.1093/nar/gkt640>.

Ma, J., Brookes, J.D., Qin, B., Paerl, H.W., Gao, G., Wu, P., et al., 2014. Environmental factors controlling colony formation in blooms of the cyanobacteria *Microcystis* spp. in Lake Taihu, China. *Harmful Algae* 31, 136–142. <https://doi.org/10.1016/j.hal.2013.10.016>.

Mathews, D.H., Disney, M.D., Childs, J.L., Schroeder, S.J., Zuker, M., Turner, D.H., 2004. Incorporating chemical modification constraints into a dynamic programming algorithm for prediction of RNA secondary structure. *Proc. Natl. Acad. Sci.* 101 (19), 7287–7292. <https://doi.org/10.1073/pnas.0401799101>.

Mathews, D.H., Turner, D.H., 2006. Prediction of RNA secondary structure by free energy minimization. *Curr. Opin. Struct. Biol.* 16 (3), 270–278. <https://doi.org/10.1016/j.sbi.2006.05.010>.

Matthew, J.H., Steffen, M.M., Gobler, C.J., Ottend, T.J., Wilhelm, S.W., Wood, S.A., Paerl, H.W., 2016. A review of the global ecology, genomics, and biogeography of the toxic cyanobacterium, *Microcystis* spp. *Harmful Algae* 54, 4–20. <https://doi.org/10.1016/j.hal.2015.12.007>.

Mcdowall, K.J., Linchao, S., Cohen, S.N., 1994. A + U content rather than a particular

- nucleotide order determines the specificity of RNase E cleavage. *J. Biol. Chem.* 269 (14), 10790–10796. [https://doi.org/10.1016/0092-8674\(94\)90243-7](https://doi.org/10.1016/0092-8674(94)90243-7).
- Merel, S., Walker, D., Chicana, R., Snyder, S., Baurès, E., Thomas, O., 2013. State of knowledge and concerns on cyanobacterial blooms and cyanotoxins. *Environ. Int.* 59, 303–327. <https://doi.org/10.1016/j.envint.2013.06.013>.
- Mikalsen, B., Boison, G., Skulberg, O.M., Fastner, J., Davies, W., Gabrielsen, T.M., et al., 2003. Natural variation in the microcystin synthetase operon *mcyABC* and impact on microcystin production in *Microcystis* strains. *J. Bacteriol.* 185 (9), 2774–2785. <https://doi.org/10.1128/jb.185.9.2774-2785.2003>.
- Mihali, T.K., Kellmann, R., Muenchhoff, J., Barrow, K.D., Neilan, B.A., 2008. Characterization of the gene cluster responsible for cylindrospermopsin biosynthesis. *Appl. Environ. Microbiol.* 74 (3), 716–722. <https://doi.org/10.1128/AEM.01988-07>.
- Morris, K.V., Mattick, J.S., 2014. The rise of regulatory RNA. *Nat. Rev. Genet.* 15 (6), 423–437. <https://doi.org/10.1038/nrg3722>.
- Ngwa, F.F., Madramootoo, C.A., Jabaji, S., 2014. Comparison of cyanobacterial microcystin synthetase (*mcyE*) gene transcript levels, *mcyE* gene copies, and biomass as indicators of microcystin risk under laboratory and field conditions. *MicrobiologyOpen* 3 (4), 411–425. <https://doi.org/10.1002/mbo3.173>.
- O'Neil, J.M., Davis, T.W., Burford, M.A., Gobler, C.J., 2012. The rise of harmful cyanobacteria blooms: the potential roles of eutrophication and climate change. *Harmful Algae* 14, 313–334. <https://doi.org/10.1016/j.hal.2011.10.027>.
- Paerl, H.W., Otten, T.G., 2013. Harmful cyanobacterial blooms: causes, consequences, and controls. *Microb. Ecol.* 65 (4), 995–1010. <https://doi.org/10.1007/s00248-012-0159-y>.
- Pearson, L., Mihali, T., Moffitt, M., Kellmann, R., Neilan, B., 2010. On the chemistry, toxicology and genetics of the cyanobacterial toxins, microcystin, nodularin, saxitoxin and cylindrospermopsin. *Mar. Drugs* 8 (5), 1650–1680. <https://doi.org/10.3390/md8051650>.
- Perez-Portel, R., Riesgo, A., 2013. Optimizing preservation protocols to extract high-quality RNA from different tissues of echinoderms for next-generation sequencing. *Mol. Ecol. Resour.* 13, 884–889. <https://doi.org/10.1111/1755-0998.12122>.
- Popenda, M., Szachniuk, M., Antczak, M., Purzycka, K.J., Lukasiak, P., Bartol, N., et al., 2012. Automated 3D structure composition for large RNAs. *Nucleic Acids Res.* 40 (14), 112. <https://doi.org/10.1093/nar/gks339>.
- Rissanen, A.J., Kurhela, E., Aho, T., Oittinen, T., Tirola, M., 2010. Storage of environmental samples for guaranteeing nucleic acid yields for molecular microbiological studies. *Appl. Microbiol. Biotechnol.* 88, 977–984. <https://doi.org/10.1007/s00253-010-2838-2>.
- Sipari, H., Rantala-Ylinen, A., Jokela, J., Oksanen, I., Sivonen, K., 2010. Development of a chip assay and quantitative PCR for detecting microcystin synthetase E gene expression. *Appl. Environ. Microbiol.* 76 (12), 3797–3805. <https://doi.org/10.1128/aem.00452-10>.
- Tillett, D., Dittmann, E., Erhard, M., Döhren, H., Börner, T., Neilan, B.A., 2000. Structural organization of microcystin biosynthesis in *Microcystis aeruginosa* PCC7806: an integrated peptide-polyketide synthetase system. *Chem. Biol.* 7 (10), 753–764. [https://doi.org/10.1016/S1074-5521\(00\)00021-1](https://doi.org/10.1016/S1074-5521(00)00021-1).
- Wolkers, W.F., Balasubramanian, S.K., Ongstad, E.L., Zec, H.C., Bischof, J.C., 2007. Effects of freezing on membranes and proteins in LNCaP prostate tumor cells. *Biochim. Biophys. Acta (BBA) - Biomembranes* 1768 (3), 728–736. <https://doi.org/10.1016/j.bbamem.2006.12.007>.
- Xia, T., SantaLucia, L.J., Burkard, M.E., Kierzek, R., Schroeder, S.J., Jiao, X., et al., 1998. Thermodynamic parameters for an expanded nearest-neighbor model for formation of RNA duplexes with Watson-Crick base pairs. *Biochemistry* 37 (42), 14719–14735. <https://doi.org/10.1021/bi9809425>.
- Xu, F., Cohen, S.N., 1995. RNA degradation in *Escherichia coli* regulated by 3' adenylation and 5' phosphorylation. *Nature* 374 (6518), 180–183. <https://doi.org/10.1038/374180a0>.
- Zuker, M., 2003. Mfold web server for nucleic acid folding and hybridization prediction. *Nucleic Acids Res.* 31 (13), 3406–3415. <https://doi.org/10.1093/nar/gkg595>.